ChemPubSoc Europe

DOI: 10.1002/cmdc.201402171

Structure-Guided Design of Thiazolidine Derivatives as *Mycobacterium tuberculosis* Pantothenate Synthetase Inhibitors

Parthiban Brindha Devi,[a] Ganesh Samala,[a] Jonnalagadda Padma Sridevi,[a] Shalini Saxena,[a] Mallika Alvala,[a] Elena G. Salina,[b] Dharmarajan Sriram,*[a] and Perumal Yogeeswari*[a]

The pantothenate biosynthetic pathway is essential for the persistent growth and virulence of *Mycobacterium tuberculosis* (*Mtb*) and one of the enzymes in the pathway, pantothenate synthetase (PS, EC: 6.3.2.1), encoded by the *panC* gene, has become an appropriate target for new therapeutics to treat tuberculosis. Herein, we report nanomolar thiazolidine inhibitors of *Mtb* PS developed by a rational inhibitor design approach. The thiazolidine compounds were discovered by using energy-based pharmacophore modelling and subsequent in vitro screening, which resulted in compounds with a half maximal inhibitory concentration (IC_{50}) value of (1.12 ± 0.12) μM. These compounds were subsequently optimised by a combination of modelling and synthetic chemistry. Hit expansion of the lead by chemical synthesis led to an improved inhibitor with an IC_{50} value of 350 nM and an *Mtb* minimum inhibitory concentration (MIC) of 1.55 μM. Some of these compounds also showed good activity against dormant *Mtb* cells.

Introduction

Tuberculosis (TB) has become one of the world's global infectious diseases. According to the World Health Organization, nearly one third of the population is infected with tuberculosis, an infectious disease that kills nearly 1.4 million people each year.[1] The current treatment for TB takes approximately six to nine months duration, which normally leads to noncompliance and, hence, the emergence of multidrug-resistant (MDR) TB and the virtually untreatable extensively drug-resistant (XDR) TB.[2] A deadly new strain of the disease was reportedly "totally drug resistant" (TDR), against which the conventional antibiotics were ineffective.[3] Therefore, there is an urgent need for new antitubercular agents with novel mechanisms of action. Pantothenate (vitamin B5), an essential precursor for the biosynthesis of coenzyme A (CoA) and acyl carrier proteins (ACPs), plays an important role in many energy and fatty acid metabolisms.[4] Microorganisms and plants synthesise pantothenate, whereas mammals obtain it from their diet. Both CoA and ACPs are essential in fatty acid biosynthesis and, for pathogenicity of *Mycobacterium tuberculosis* (*Mtb*), pantothenate synthetase (PS) could be an appropriate target for developing new drugs against TB. It has been reported that an auxotrophic mutant of *Mtb* that is defective in the de novo biosynthesis of pantothenate was highly attenuated, both in immunocompromised and immunocompetent mice. This indicated that a functional pantothenate biosynthetic pathway was essential for the virulence of *Mtb*.[5] In the present study, we used the crystal structure of the *Mtb* PS in complex with pantoyl adenylate as a template for energy-based pharmacophore (e-pharmacophore) modelling and docking to identify novel small molecules as putative active site ligands. The compound 3-({5-[2-(carboxymethoxy)benzylidene]-3-methyl-4-oxo-1,3-thiazolidin-2-ylidene}amino)benzoic acid was identified as a strong inhibitor of *Mtb* PS with a half maximal inhibitory concentration (IC_{50}) value of (1.12 ± 0.12) μM and was further investigated for structure–activity relationship (SAR) studies. An outline of the work used for identifying the inhibitors has been depicted in Figure 1.

Results and Discussion

We used the crystal structure of PS from *Mtb* in complex with the reaction intermediate pantoyl adenylate (Protein Data Bank ID: 1N2I) with 1.7 Å resolution[6] (provided as Figure S1 in the Supporting Information), although there are many other crystal structures published in the Protein Data Bank (http://www.rcsb.org/pdb) for PS in complex with α,β-methyleneadnosine 5′-triphosphate (AMPCPP), pantoate,[6] adenosine monophosphate (AMP), adenosine triphosphate (ATP)[7] and various ligands and fragments developed by fragment-based design,[8–10] with resolutions ranging from 1.6 to 2.33 Å. We attempted to employ a new drug design strategy for PS based

[a] P. B. Devi, G. Samala, J. P. Sridevi, S. Saxena, M. Alvala, Prof. D. Sriram, Prof. P. Yogeeswari
Drug Discovery Research Laboratory, Department of Pharmacy
Birla Institute of Technology and Science-Pilani
Hyderabad Campus, Hyderabad-500078 (India)
E-mail: dsriram@hyderabad.bits-pilani.ac.in
pyogee@hyderabad.bits-pilani.ac.in

[b] E. G. Salina
Institution of the Russian Academy of Sciences
A.N. Bach Institute of Biochemistry RAS, Moscow (Russia)

Supporting information for this article is available on the WWW under http://dx.doi.org/10.1002/cmdc.201402171: detailed experimental procedures used for docking and interaction profiles and results for the active analogues.

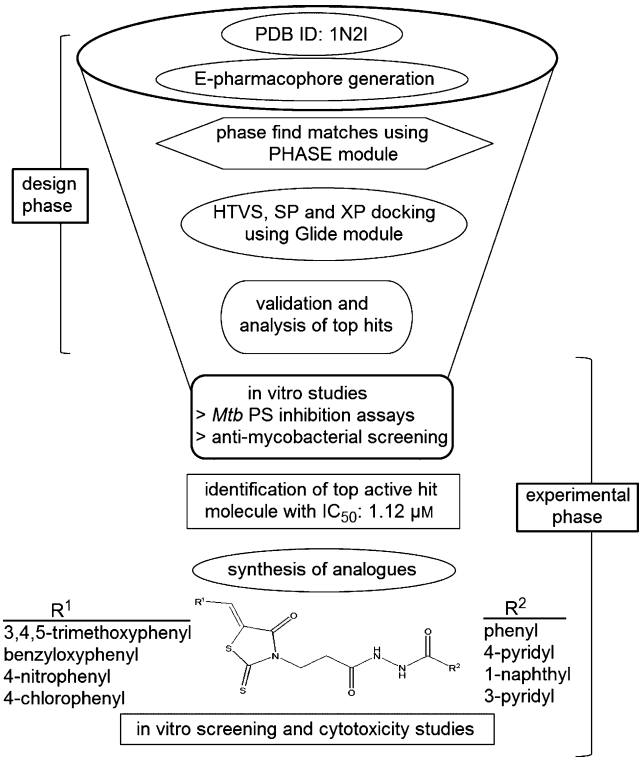

Figure 1. Outline of the computational and experimental work presented in this study.

on structure-based e-pharmacophore modelling, which had not been explored for this target, so we started with the reaction intermediate pantoyl adenylate because it is crucial in the enzyme action. An initial validation of the active site pocket was performed by redocking the crystal ligand pantoyl adenylate with the active site residues of the *Mtb* PS protein. The redocking results showed that the compound exhibited similar interactions to those of the original crystal structure, which was further confirmed with a root mean square deviation (RMSD) of 0.312 Å. The pantoyl adenylate reference ligand showed hydrogen-bonding interactions with the Val187, Met195, Gln164, Met40, His47, Gly158, Gln72 and Asp161 amino acid residues, which were retained with the redocked ligand. Pharmacophore hypotheses based on mapping of the energetic terms from the extra precision (XP) Glide scoring function onto the atom centres were obtained by using Phase software.[11,12] The number of pharmacophore sites was set to ten and the total number of pharmacophore sites derived was six, with four acceptors (A) and two donors (D).[13] The six-point e-pharmacophore hypothesis (Figure S2 in the Supporting Information) was then used for the virtual screening of a commercial database (Asinex).[14]

Compounds retrieved by the e-pharmacophore filter by using the Phase software with a fit value above 1.5 were regarded as potential hits and were carried forward for high-throughput virtual screening (HTVS). The virtual screening options for HTVS, standard precision (SP) and Glide XP docking, were executed. Compounds resulting in a score of ≤ -6.0 kcal mol^{-1} and three or more hydrogen bonds were subjected to another round of docking with Glide XP.[15] Glide XP combined accurately physics-based scoring terms and thorough sampling and resulted in compounds with docking scores between -9.649 and -6.222 kcal mol^{-1}.[16,17] Although the docking score did not indicate the compound's binding affinity, it was helpful in distinguishing active compounds from inactive ones. The final shortlisting of hit compounds was based on visual inspection of the important amino acid residues involved in binding, which included hydrogen bonding with Val187, Met195, Met40, Gln164, Gln72, Gly158 and Asp161 and π–π stacking interactions with Hie44 and Hie47 (Hie: the protonated state of histidine with a hydrogen atom at the ε position). The selected hits (41 compounds from 500 000 compounds) retrieved from the commercial database (Asinex) were experimentally screened against *Mtb* PS at various concentrations and the IC_{50} values were calculated by using GraphPad Prism analysis software.

Seven compounds showed $>60\%$ inhibition at 25 μM concentration and the IC_{50} values are reported in Figure 2. As shown in Figure 2, (*Z*)-*N*′-(3-(5-(benzo[*d*][1,3]dioxol-5-ylmethy-

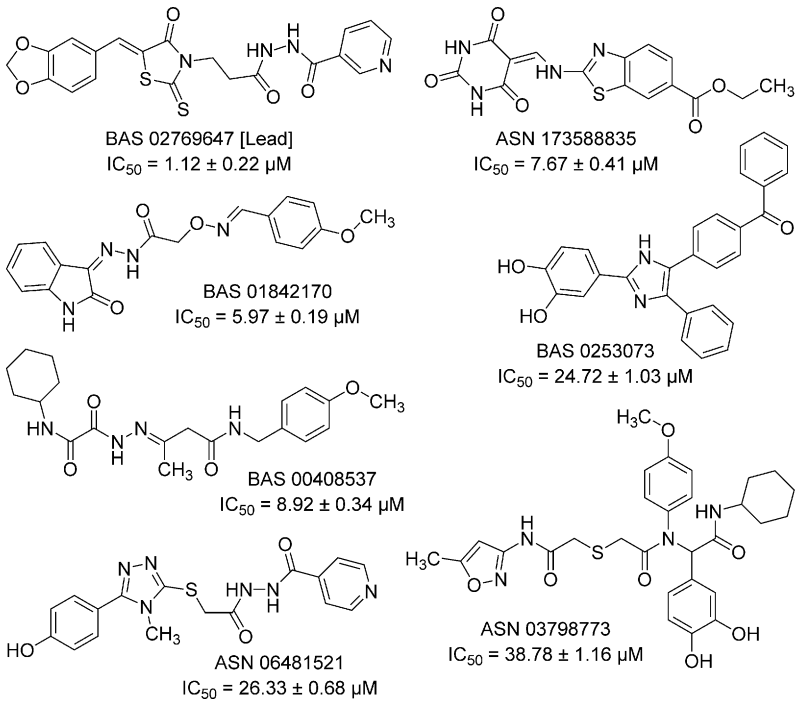

Figure 2. Top seven Asinex database hit molecules and their *Mtb* PS IC_{50} values.

lene)-4-oxo-2-thioxothiazolidin-3-yl)propanoyl)nicotinohydrazide (**Lead**) was found to be the most potent inhibitor with an IC_{50} value of (1.12±0.12) μM. With the aim of getting insight into the structural basis for its activity, this compound was analysed in more detail. The compound was found to display the highest docking score among the other identified Asinex hits, with a docking score of −7.089 kcal mol^{-1}. The lead compound was found to be associated with four hydrogen-bonding interactions with relevant amino acid residues of the protein (Figure 3). An oxygen atom of the benzodioxo group was found to interact with Val187. The oxygen atom and NH moiety of the carbohydrazide group attached to the pyridyl end were found to be associated with Gln164 and the carbonyl oxygen atom on the thiazole ring participated in hydrogen bonding with Hie47, an interaction analogous to the one observed in the crystal ligand with His44. In addition to hydrogen-bonding interactions, the 3-pyridyl ring was found to be well placed in the hydrophobic pocket consisting of Phe67, Val142, Leu146 and Pro38. Apart from the hydrophobic interactions, the 3-pyridyl ring showed polar contacts with Asn69, Gln72, Ser65 and Thr39, whereas the 5-benzo[*d*][1,3]dioxo moiety showed polar contacts with Hie47, Ser196 and Thr186 and was also involved in hydrophobic interactions with Met195, Ala49, Leu50 and Val184. The orientation of the lead compound was also found to be similar to that of the crystal ligand (Figure S1 in the Supporting Information).

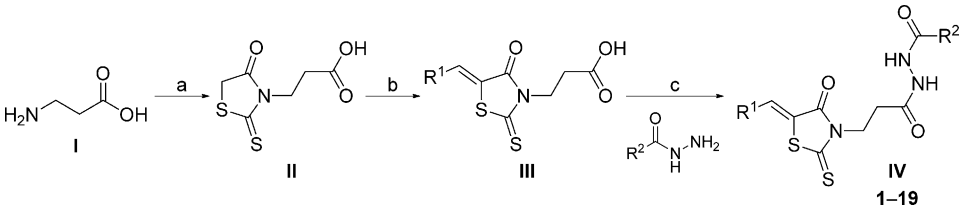

Scheme 1. Synthetic protocol for the compounds. *Reagents and conditions*: a) KOH, CS_2, $BrCH_2COOH$, H_2O, RT, 9 h; b) R^1CHO, piperidine, EtOH, reflux, 6 h; c) EDCI, HOBt, Et_3N, DMF, RT, 7 h. EDCI: 3-(3-dimethylaminopropyl)-1-ethylcarbodiimide; HOBt: 1-hydroxy-1*H*-benzotriazole.

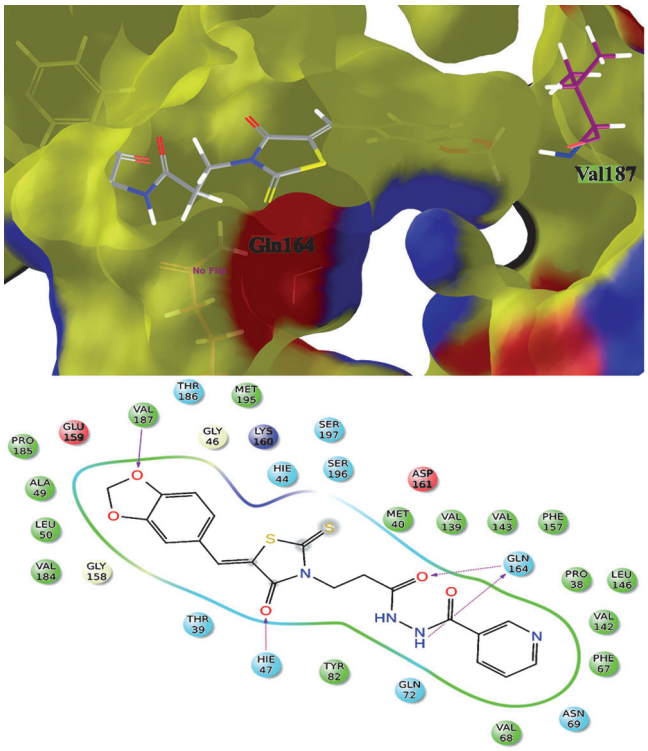

Figure 3. Binding pose and interaction pattern of the lead molecule.

To study the SAR of the lead compound, we further synthesised 19 compounds and assayed them for *Mtb* PS inhibition. The synthetic pathway employed to achieve the target compounds has been delineated in Scheme 1. The final compounds were synthesised in three steps: in the first step, β-alanine (**I**) was treated with carbon disulfide and bromoacetic acid under basic conditions with water as the solvent to form compound **II** in good yield (81%).[18] Compound **II** was then subjected to a Knoevenagel type condensation with different aldehydes by heating at reflux in ethanol with a catalytic amount of piperidine to achieve compounds **III** in excellent yields (90%). Finally compounds **III** were treated with acid hydrazides by using EDCI, HOBt and Et_3N at room temperature to yield compounds **1**–**19**. Initially, we tried to synthesise compound **III**in three steps by starting with the condensation of rhodanine and 4-chlorobenzaldehyde to give 5-(4-chlorobenzylidene)-2-thioxothiazolidin-4-one, followed by a later reaction with ethyl-3-bromoacetate to form ethyl 3-(5-(4-chlorobenzylidene)-4-oxo-2-thioxothiazolidin-3-yl)propanoate and hydrolysis of the ester in a third step to afford compounds **III**. Due to low yields in steps 1 and 2 and the poor solubility of the step 2 product, we did not adopt this synthetic route to proceed further.

Synthesised compounds were assayed in an *Mtb* PS inhibition study that couples the AMP produced in the condensation of β-alanine and pantoate with the oxidation of reduced nicotinamide adenine dinucleotide (NADH) to NAD^+ through myokinase, pyruvate kinase and lactate dehydrogenase.[19] The decrease in the absorbance of NADH was spectrophotometrically monitored at 340 nm. In the initial screening at 25 μM, all of the compounds showed more than 50% inhibition against *Mtb* PS and their IC_{50} values were calculated for various concentrations as described previously. The IC_{50} values were found to be in the range of (0.35±0.01) to (5.86±0.11) μM (Table 1). Five compounds (**9**, **12**, **13**, **16** and **19**) were found to more effective with IC_{50} values less than 1 μM. Compound **9** emerged as the most active compound, with an IC_{50} value of (0.35±0.01) μM. To confirm the specific inhibition of PS separately from the other "coupled enzymes" in the assay, the hits were tested in an assay that was performed as above except that the final concentration of lactate dehydrogenase was 0.2 units mL^{-1} and no pantoic acid was added to the reaction mixture. The "coupled enzyme" assay was initiated with AMP (6.5 mM final concentration) instead of PS.

Table 1. Biological activities of the synthesised compounds.

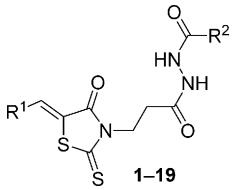

1–19

Compd	R^1	R^2	IC_{50} [μM][a]	MIC [μM] H37 Rv[b]	MIC [μM] Verap.[c]	MIC [μM] Piper.[c]	Cytotoxicity [%][d]
lead	5-benzo[*d*][1,3]dioxole	3-pyridyl	1.12 ± 0.12	54.81	13.70	27.40	38.92 ± 0.12
1	5-benzo[*d*][1,3]dioxole	phenyl	5.86 ± 0.11	54.95	13.73	13.73	63.22 ± 0.26
2	5-benzo[*d*][1,3]dioxole	4-pyridyl	1.21 ± 0.07	54.82	27.41	27.41	36.55 ± 0.38
3	5-benzo[*d*][1,3]dioxole	1-naphthyl	1.05 ± 0.03	24.75	3.09	12.37	61.80 ± 0.22
4	4-chlorophenyl	phenyl	4.89 ± 0.02	56.18	7.02	3.51	62.58 ± 1.02
5	4-chlorophenyl	4-pyridyl	3.50 ± 0.03	56.05	14.01	7.00	42.11 ± 0.65
6	4-chlorophenyl	1-naphthyl	1.17 ± 0.02	25.25	12.62	25.25	63.71 ± 2.92
7	4-chlorophenyl	3-pyridyl	1.35 ± 0.03	7.01	7.01	3.50	50.62 ± 3.32
8	3,4,5-trimethoxyphenyl	phenyl	1.39 ± 0.22	6.24	1.56	3.12	45.37 ± 0.33
9	3,4,5-trimethoxyphenyl	4-pyridyl	0.35 ± 0.01	1.55	0.38	0.77	22.21 ± 0.65
10	3,4,5-trimethoxyphenyl	1-naphthyl	1.14 ± 0.04	5.67	5.67	5.67	56.17 ± 0.62
11	3,4,5-trimethoxyphenyl	3-pyridyl	2.12 ± 0.03	49.80	6.22	24.9	35.37 ± 0.26
12	4-nitrophenyl	phenyl	0.37 ± 0.02	1.71	0.85	0.85	50.05 ± 0.53
13	4-nitrophenyl	4-pyridyl	0.59 ± 0.03	13.68	13.68	13.68	21.78 ± 0.47
14	4-nitrophenyl	1-naphthyl	1.40 ± 0.03	12.35	1.54	1.54	41.23 ± 0.66
15	4-nitrophenyl	3-pyridyl	2.51 ± 0.02	3.41	0.85	0.85	32.92 ± 0.29
16	4-benzyloxyphenyl	phenyl	0.79 ± 0.03	24.18	24.18	12.09	43.96 ± 1.05
17	4-benzyloxyphenyl	4-pyridyl	1.54 ± 0.03	24.13	6.03	6.03	53.05 ± 2.23
18	4-benzyloxyphenyl	1-naphthyl	1.70 ± 0.01	88.18	22.04	44.09	27.22 ± 0.64
19	4-benzyloxyphenyl	3-pyridyl	0.51 ± 0.02	12.07	12.07	12.07	28.20 ± 0.93
isoniazid			> 25	0.72	0.72	0.72	NT
ethambutol			> 25	7.64	7.64	3.82	NT

[a] Against the *Mtb* PS enzyme. Results are given as the mean ± S from $n = 3$ experiments. [b] Minimum inhibitory concentration (MIC) against *M. tuberculosis* H37 Rv cells. [c] MIC against *M. tuberculosis* H37 Rv cells in the presence of verapamil (Verap.) or piperine (Piper.). [d] Percent inhibition of RAW 264.7 cell growth with test compounds at a concentration of 100 μM. Results are given as the mean ± SD from $n = 3$ experiments; NT: not tested.

The synthesised compounds were docked to *Mtb* PS in order to support the structure–activity relationship. Firstly, the R^1 position of the parent compound was substituted with 4-chlorophenyl, 3,4,5-trimethoxyphenyl, 4-nitrophenyl and 4-benzyloxyphenyl groups. Of these derivatives, compounds with 3,4,5-trimethoxyphenyl (**8**–**11**), benzyloxyphenyl (**16**–**19**) or 4-nitrophenyl (**12**–**15**) groups showed good activities ((0.35 ± 0.013)–(2.51 ± 0.024) μM) relative to those with a 4-chlorophenyl group ((1.17 ± 0.027)–4.89 ± 0.019) μM). Replacement of the benzo(*d*)[1,3]dioxole with a 3,4,5-trimethoxyphenyl or benzyloxyphenyl group at the R^1 position had an important effect on the enzyme activity. The assay results confirmed that the molecule with a 3,4,5-trimethoxyphenyl group at the R^1 position, **9**, was more active than the benzyloxyphenyl-containing compound **19**. This could be attributed to the presence of an extra cation–π interaction between His47 and the phenyl group of the molecule. Substitution at the R^1 position with a nitrophenyl group (**12**–**15**) showed better activity. Compound **12** showed high activity in the *Mtb* PS assay ((0.37 ± 0.018) μM). This can be supported by the strong nonpolar interactions in the hydrophobic pocket and a cationic interaction between the oxygen atom of the nitro group and Lys160. Further substitution of 4-nitrophenyl-containing compounds at the R^2 position with phenyl, 4-pyridyl, 1-naphthyl and 3-pyridyl moieties showed a decrease in the activity range, which suggests that the phenyl substitution is the appropriate one. Compounds with a chlorophenyl group at the R^1 position (**4**–**7**) were found to be less active with an IC_{50} range of (1.17 ± 0.027)–(4.89 ± 0.019) μM. The orientations of these compounds were found to be different from those of the remaining compounds, probably because of the highly electronegative nature.

Compounds **1**–**3**, substituted at the R^2 position with phenyl, 4-pyridyl and 1-naphthyl groups, differ in their activity ranges. By comparing the orientation of these molecules at their active site, it was found that the 4-pyridyl and 1-naphthyl moiety were in the hydrophobic pocket, whereas the compound with phenyl substitution, **1**, was facing toward the solvent, which explained its low activity profile. Compounds **3**, **6**, **10**, **14** and **18** with 1-naphthyl substitution at the R^2 position showed slightly better or equipotent activity (IC_{50} = 1.05–1.70 μM) to that of lead compound (IC_{50} = 1.12 μM). This was well supported by the interaction profiles in the docking studies, with the compounds orienting in a similar manner to the crystal ligand and retaining three–four hydrogen bonds, as observed with the reference molecule (Hie44, Asp161, Val187, Ser126 and Ser127). However, replacement with a phenyl group at the R^2 position (compound **1**) led to a fivefold decrease in activity (IC_{50} = 5.86 μM), which was analysed from the interaction pro-

file as being due to the molecule taking a slightly different orientation/pose that excluded the hydrophobic interactions. The binding pose and interaction pattern of this molecule are depicted in Figure S4 in the Supporting Information.

Compounds **4**–**7**, with a 4-chlorophenyl group at the R^1 position and with the R^2 position substituted with four different aryl rings, resulted in activities in the range from 1.17 to 4.89 μM. Compounds **6** and **7**, with R^2-substituted 1-naphthyl and 3-pyridyl groups, respectively, showed good activity with IC_{50} values of 1.17 and 1.35 μM, respectively. Compound **6** was associated with three hydrogen-bonding interactions with relevant amino acids and was further stabilised by a cation–π interaction with Arg181. The 4-chlorophenyl group was inserted into the hydrophobic cavity lined by Met40, Val187, Ala49, Pro185, Val184 and Leu50.

When the R^1 position was substituted with a 4-benzyloxyphenyl group, two nanomolar inhibitors, **16** and **19**, emerged, with IC_{50} values of 0.79 and 0.51 μM, respectively. These compounds revealed hydrogen bonding with Hie47, Val187, Hie44, Ser196 and Met195 and the 4-benzyloxyphenol group was buried in the hydrophobic pocket with Val143, Val142, Phe157, Val139, Val68 and Phe67. Thus, a bulkier group at the R^1 position was favourable for PS inhibition.

Overall, compound **9** emerged as the most potent inhibitor of *Mtb* PS with a low IC_{50} value of 0.35 μM. Closer analysis of compound **9** in the binding site revealed four hydrogen bonds; the carbonyl oxygen atom on the thiazolidine ring showed hydrogen bonding with Ser196 and Ser197 and the NH group on the acid hydrazide participated with Asp161 and was further stabilised by a cation–π stacking interaction with Arg198 (Figure S3 in the Supporting Information). The 3,4,5-trimethoxyphenyl group at the R^1 position occupied the hydrophobic pocket surrounded by Pro157, Pro185, Ala49, Ala194, Val184, Val187, Phe157, Leu50 and Met195. However, the good PS potency of this compound could be explained by these hydrophobic interactions only if the 3,4,5-trimethoxyphenyl core remained in the hydrophobic pocket which was earlier demonstrated to be crucial for activity.[6]

Furthermore, all of the compounds were screened for their in vitro anti-mycobacterial activity against a log phase culture of *M. tuberculosis* H37Rv by the microplate Alamar blue assay (MABA) method for the determination of the minimum inhibitory concentration (MIC) in duplicate.[20] The MICs of the synthesised compounds along with the standard drugs for comparison are presented in Table 1. The compounds showed MICs in the range of 1.55–88.18 μM and six compounds showed promising activity with MICs of less than 10 μM. Relative to the standard first-line antitubercular drug ethambutol (MIC = 7.64 μM), six compounds were found to be more active, but they were found to be less active than isoniazid (MIC = 0.72 μM). Among the compounds tested, compound **9** was found to be the most active in vitro with an MIC of 1.55 μM. Most of the molecules that showed good *Mtb* PS enzyme inhibition did not exhibit equally potent inhibition against *Mtb*. This could be due to the involvement of a wide array of efflux mechanisms mediated by several ATP-binding cassette (ABC) transporters and major facilitator superfamily (MFS) proteins or antibiotic-modifying and -degrading enzymes, to name a few possibilities.[21] Multiple drugs, like verapamil, reserpine, piperine and phenothiazines such as thioridazine, have been shown to inhibit bacterial efflux pumps in vitro.[22] Several models have been proposed,[23] such as 1) direct binding and inhibition of pump assembly or function, 2) disruption of the transmembrane gradients used by secondary transporters, 3) inhibitor binding to the antimicrobial compound, and 4) competition for efflux. As a hypothesis, we tested all of the compounds for their MIC change in the presence of the reported efflux pump inhibitors verapamil and piperine and in most cases, except **13**, **16** and **19** (Table 1), the potency improved by two- to six-fold relative to that in the absence of efflux pump inhibitors. Interestingly, these three compounds were among the five most potent PS inhibitors that showed IC_{50} values of less than 1 μM. Further investigations on other parameters like lipophilicity or polarity could reveal further information on the antitubercular activity of these compounds. The most active compound, **9**, showed an MIC of 0.38 μM, which is twice as potent than isoniazid. This experiment was an indication that the efflux mechanism could be an important hurdle in the antitubercular efficacy of novel drugs.

Furthermore, a few promising compounds (**9**, **12** and **15**) were tested for their *Mtb* MICs in the presence of 1% and 5% pantothenic acid and there were no differences in the MICs under the different conditions. In earlier reports, the *panCD* knockouts were able to grow in SCID and BALB/C mice, albeit with greatly attenuated virulence.[5] The authors suggested an unidentified permease was salvaging enough pantothenate for survival but not enough to cause disease. In order for a pantothenate biosynthesis inhibitor to be effective, the supply of exogenous pantothenate must be exhausted. Hence, in our study, we observed that up to 5% supplementation of pantothenic acid did not cause any activity difference. Further extensive study based on daily intake in animal models or based on overexpression of PS might yield clear understanding. Also, by generating resistant mutants followed by whole genome sequencing to identify resistance, mutations could also be evaluated.

Compounds **9**, **12** and **19** were also examined for their activity against dormant "non-culturable" *Mtb* bacilli at 20 and 100 μM. "Non-culturable" cells obtained with low metabolic activity were characterised by marked phenotypic resistance to both isoniazid and rifampicin and were unable to form colonies on agar-solidified Sauton's medium but could be reactivated in liquid medium after special procedures of resuscitation.[24] Thus, these cells met the key criteria of dormancy and could be applied as a relevant tool for finding drugs for latent TB. For estimation of the inhibitory effect of the compounds, the concentrations of both treated and untreated "non-culturable" cells recovered from dormancy were estimated by most probable number (MPN) assay with the use of statistical approaches.[24] It was found that, after treatment with compounds **9** and **12**, the dormant "non-culturable" cells were less able to recover from dormancy (Figure 4). Compound **12** at 20 μM caused an approximately one-log decrease in the viability of dormant cells after incubation for seven days. Although

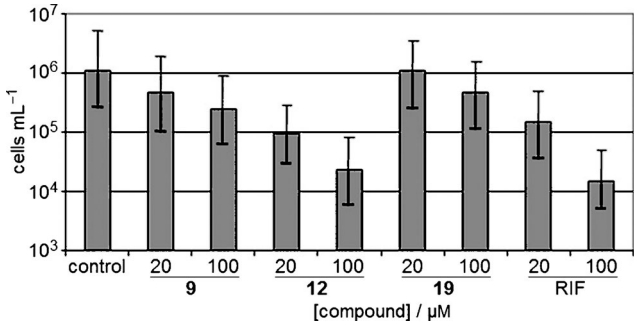

Figure 4. The effectiveness of compounds **9**, **12**, and **19** in killing *M. tuberculosis* dormant "non-culturable" cells. "Non-culturable" cells were washed and treated with 20 or 100 μM rifampicin (RIF) or test compounds for seven days. The viability of both treated and untreated "non-culturable" cells was determined from the concentration of cells that were able to recover from the dormant "non-culturable" state by the MPN assay. Error bars represent 95% confidence limits.

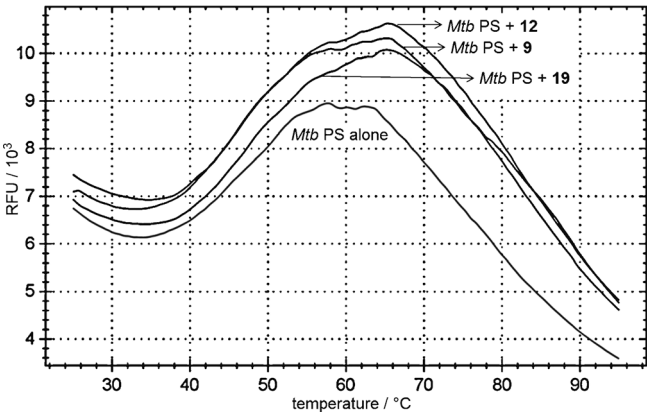

Figure 5. DSF experiment for compounds **9**, **12**, and **19**, showing an increase in thermal stability between the native *Mtb* PS protein and the *Mtb* PS protein–compound complexes.

this effect was quite a modest one, the activity of this compound was similar to that of rifampicin in relation to dormant *Mtb*. These compounds may be regarded as the prominent ones for the development of derivatives that are more effective for dormant *Mtb* cells and latent TB. Pantothenate is an essential precursor for the biosynthesis of acetyl-coenzyme A, which is a central intermediate in primary metabolism with roles in the tricarboxylic acid (TCA) cycle, as well as fatty acid and amino acid biosynthesis. The flux of carbon through acetyl-coenzyme A is particularly critical to non-replicating *Mtb*.[25] Fatty acids, through the breakdown to acetyl-coenzyme A and use of the glyoxylate shunt, provided carbon for carbohydrate synthesis and, thus, acetyl-coenzyme A appears to be a gate through which much of the used carbon pool passes.

The synthesised compounds were also tested for in vitro cytotoxicity against RAW 264.7 (mouse macrophage) cells at 100 μM concentration by using a 3-(4,5-dimethylthiaol-2-yl)-2,5-diphenyltetrazolium bromide (MTT) assay.[26] We used RAW 264.7 (mouse macrophage) cells because the *Mtb* bacterium resides inside macrophages. The monocyte macrophage (RAW 264.7) cell lines are mostly used for tuberculosis research and compound toxicity studies. The percentage inhibition is reported in Table 1. Compounds inhibited in the range of 21.78–63.71%. The most promising compound, **9**, showed only 22.21% cytotoxicity at 100 μM and the selectivity index was >64.

The interaction of the top active leads (**9**, **12** and **19**) with the protein and their ability to stabilise the protein were evaluated by measuring the fluorescence of a dye in the presence of the native protein and protein–ligand complexes by using the differential scanning flourimetry (DSF) technique. It measures the thermal stability of a target protein and a subsequent increase in protein melting temperature (T_m) would indicate binding of a ligand to the protein.[27] A positive shift of the T_m value corresponding to the native protein indicates increased stability due to inhibitor binding. Figure 5 shows the melting curves with compounds **9**, **12** and **19**. The *Mtb* PS protein showed a melting temperature of 52.50 °C, whereas the corresponding T_m values in the presence of compounds **9**, **12** and **19** were found to be 56.80, 56.70 and 58.20 °C, respectively. This study revealed that these compounds bind to the enzyme, which was indicated by the increased protein stability. Furthermore, this study indicated that these compounds could be further developed as valuable drug candidates against *Mtb* PS.

Conclusion

In the present study, structure-based e-pharmacophore modelling was employed to identify structurally diverse, small-molecule inhibitors of the *Mtb* PS enzyme based on the crystal structure co-crystallised with an inhibitor. Seven active compounds from varied structural classes were identified, out of which four molecules showed *Mtb* PS activity with $IC_{50}<$ 10 μM, and the best compound was selected as the lead to further synthesise a library of 19 molecules. All of these compounds were subjected to an *Mtb* PS inhibition assay. Furthermore, the binding and enhanced protein stability of some compounds was biophysically confirmed by DSF. It is gratifying to report that the best inhibitory compounds, **9** and **12**, showed a greater positive shift in the DSF results, which indicates an increase in thermal stability of the inhibitor–protein complex that correlates well with the in vitro antitubercular activity as well. Furthermore, compounds **9** and **12** showed better activity against dormant *Mtb*, which makes these compounds a potential chemical class to develop as *Mtb* PS inhibitors.

Experimental Section

Chemistry

Preparation of 3-(4-oxo-2-thioxothiazolidin-3-yl)propanoic acid (II): 30% Aqueous KOH (26.3 mL, 141.2 mmol) was added dropwise to a stirred solution of compound **I** (7.0 g, 78.65 mmol) in H_2O (30 mL) at 0 °C, then CS_2 (6.57 g, 86.52 mmol) was added dropwise to the reaction mixture at the same temperature. The mixture was

allowed to stir at room temperature for 3 h, then bromoacetic acid (10.8 g, 78.65 mmol) was added as a solid in small portions over about 20 min. The reaction was allowed to mix at room temperature for an additional 3 h, during which time a precipitate formed. The pH value of the reaction mixture was adjusted to 3–4 with concd H_2SO_4 and the mixture was stirred for 1 h. The product was filtered off, washed with water and dried in a vacuum oven to get compound **II** as an off-white solid (9.7 g, 60%): ^{1}H NMR (300 MHz, $CDCl_3$): $\delta = 2.50$ (t, $J = 7.6$ Hz, 2H), 4.30 (s, 2H), 4.32 (t, $J = 7.6$ Hz, 2H), 12.45 ppm (s, 1H); MS (ES, 70 eV): *m/z* 206 $[M+H]^+$.

General procedure for the preparation of compound III: Aldehyde (1.0 equiv), compound **II** (1.0 equiv) and piperidine (catalytic) were mixed in EtOH and stirred under reflux conditions for 6 h. The reaction mixture was concentrated under reduced pressure and the obtained solid compound was filtered and washed with hexanes to get compound **III**.

Preparation of (*Z*)-3-(5-(benzo[*d*][1,3]dioxol-5-ylmethylene)-4-oxo-2-thioxothiazolidin-3-yl)propanoic acid: Piperonal (2.19 mL, 14.63 mmol) and piperidine (catalytic) were added to a stirred solution of compound **II** (3.0 g, 14.63 mmol) in EtOH (25 mL) at room temperature and heated at reflux for 6 h. The reaction mixture was concentrated under reduced pressure and the obtained solid compound was filtered off and washed with hexanes to get the title compound as an off-white solid (4.5 g, 91%): ^{1}H NMR (300 MHz, [D$_6$]DMSO): $\delta = 2.70$ (t, $J = 7.6$ Hz, 2H), 4.39 (t, $J = 7.6$ Hz, 2H), 6.30 (s, 2H), 6.90 (d, $J = 7.2$ Hz, 1H), 7.23 (d, $J = 7.6$ Hz, 1H), 7.27 (s, 1H), 7.9 (s, 1H), 12.54 ppm (s, 1H); MS (ES, 70 eV): *m/z* 338 $[M+H]^+$.

General procedure for the preparation of compound IV: EDCI (1.3 equiv), HOBt (1.3 equiv) and Et_3N (2.2 equiv) were added to a stirred solution of compound **III** (1.0 equiv) in CH_2Cl_2 at 0 °C. The reaction mixture was stirred for few minutes, then $R_2CONHNH_2$ (1.2 equiv) was added and the reaction mixture was allowed to stir at room temperature for 4 h. The solids formed in the reaction mixture were filtered off and washed with H_2O, hexanes and diethyl ether. The obtained solid compound was dried in vacuum oven to get compound **IV**.

(*Z*)-*N*′-(3-(5-(Benzo[*d*][1,3]dioxol-5-ylmethylene)-4-oxo-2-thioxothiazolidin-3-yl)propanoyl)benzohydrazide (1): EDCI (0.22 g, 1.15 mmol), HOBt (0.16 g, 1.15 mmol) and Et_3N (0.28 mL, 1.96 mmol) were added to a stirred solution of (*Z*)-3-(5-(benzo[*d*]-[1,3]dioxol-5-ylmethylene)-4-oxo-2-thioxothiazolidin-3-yl)propanoic acid (0.3 g, 0.89 mmol) in CH_2Cl_2 (4 mL) at 0 °C. The reaction mixture was stirred for a few minutes, then benzohydrazide (0.15 g, 1.06 mmol) was added and the reaction mixture was allowed to stir at room temperature for 4 h. The solids formed in the reaction mixture were filtered off and washed with H_2O (3×20 mL), hexanes and diethyl ether. The solid compound was dried in a vacuum oven to get the title compound as an off-white solid (0.35 g, 87%): mp: 231–232 °C; ^{1}H NMR (400 MHz, [D$_6$]DMSO): $\delta = 2.79$ (t, $J = 7.2$ Hz, 2H), 4.41 (t, $J = 7.2$ Hz, 2H), 6.42 (s, 2H), 7.27 (d, $J = 6.8$ Hz, 1H), 7.54 (s, 1H), 7.54–7.63 (m, 3H), 7.81–7.92 (m, 4H), 9.70 ppm (br s, 2H); ^{13}C NMR (100 MHz, [D$_6$]DMSO): $\delta = 37.6$, 47.5, 102.0, 108.2, 115.0, 126.6 (2C), 127.1, 128.3 (2C), 129.2, 132.4, 142.2, 142.7, 147.7, 148.3, 149.9, 164.6, 165.6, 179.4, 189.2 ppm; MS (ES, 70 eV): *m/z* 456 $[M+H]^+$; elemental analysis: calcd (%) for $C_{21}H_{17}N_3O_5S_2$: C 55.37, H 3.76, N 9.22; found: C 55.41, H 3.79, N 9.27.

(*Z*)-*N*′-(3-(5-(Benzo[*d*][1,3]dioxol-5-ylmethylene)-4-oxo-2-thioxothiazolidin-3-yl)propanoyl)isonicotinohydrazide (2): Yield: 91%; mp: 260–261 °C; ^{1}H NMR (400 MHz, [D$_6$]DMSO): $\delta = 2.62$ (t, 2H), 4.71 (t, $J = 7.2$ Hz, 2H), 6.62 (s, 2H), 7.47 (d, $J = 7.2$ Hz, 1H), 7.62–7.72 (m, 3H), 7.72 (s, 1H), 7.90–8.10 (m, 3H), 9.72 ppm (br s, 2H); ^{13}C NMR (100 MHz, [D$_6$]DMSO): $\delta = 188.6$, 172.6, 168.3, 164.6, 151.9, 148.4 (2C), 147.2, 141.9, 141.2, 133.9, 128.7, 126.7 (2C), 125.4, 119.0, 108.7, 101.7, 49.7, 38.3 ppm; MS (ES, 70 eV): *m/z* 457 $[M+H]^+$; elemental analysis: calcd (%) for $C_{20}H_{16}N_4O_5S_2$: C 52.62, H 3.53, N 12.27; found: C 52.71, H 3.61, N 12.31.

(*Z*)-*N*′-(3-(5-(Benzo[*d*][1,3]dioxol-5-ylmethylene)-4-oxo-2-thioxothiazolidin-3-yl)propanoyl)-1-naphthohydrazide (3): Yield: 88%; mp: 249–250 °C; ^{1}H NMR (400 MHz, [D$_6$]DMSO): $\delta = 2.57$ (t, $J = 8.4$ Hz, 2H), 4.77 (t, $J = 8.8$ Hz, 2H), 6.59 (s, 2H), 7.49 (s, 1H), 7.53–7.74 (m, 2H), 7.89 (d, $J = 7.6$ Hz, 2H), 8.21–8.91 (m, 6H), 10.21 ppm (br s, 2H); ^{13}C NMR (100 MHz, [D$_6$]DMSO): $\delta = 36.3$, 45.9, 108.7, 121.6, 123.4, 124.6, 125.4, 126.9, 127.4, 128.7, 129.4, 132.1, 132.8, 133.0, 133.9, 142.0, 142.5, 147.3, 148.8, 149.1, 151.9, 165.0, 165.3, 177.6, 190.6 ppm; MS (ES, 70 eV): *m/z* 506 $[M+H]^+$; elemental analysis: calcd (%) for $C_{25}H_{19}N_3O_5S_2$: C 59.39, H 3.79, N 8.31; found: C 59.41, H 3.82, N 8.37.

(*Z*)-*N*′-(3-(5-(4-Chlorobenzylidene)-4-oxo-2-thioxothiazolidin-3-yl)propanoyl)benzohydrazide (4): Yield: 79%; mp: 246–247 °C; ^{1}H NMR (400 MHz, [D$_6$]DMSO): $\delta = 2.44$ (t, $J = 7.6$ Hz, 2H), 4.18 (t, $J = 7.6$ Hz, 2H), 7.31 (d, $J = 6.8$ Hz, 2H), 7.42 (s, 1H), 7.56–7.69 (m, 5H), 7.80 (d, $J = 6.8$ Hz, 2H), 9.60 (s, 1H), 9.70 ppm (s, 1H); ^{13}C NMR (100 MHz, [D$_6$]DMSO): $\delta = 37.1$, 45.7, 125.7 (2C), 126.1 (2C), 127.1 (2C), 128.2 (2 C), 130.2, 133.6, 135.8, 136.7, 142.3, 146.9, 169.6, 177.6, 178.4, 188.2 ppm; MS (ES, 70 eV): *m/z* 446 $[M+H]^+$; elemental analysis: calcd (%) for $C_{20}H_{16}ClN_3O_3S_2$: C 53.87, H 3.62, N 9.42; found: C 54.01, H 3.69, N 9.47.

(*Z*)-*N*′-(3-(5-(4-Chlorobenzylidene)-4-oxo-2-thioxothiazolidin-3-yl)propanoyl)isonicotinohydrazide (5): Yield: 72%; mp: 259–260 °C; ^{1}H NMR (400 MHz, [D$_6$]DMSO): $\delta = 2.25$ (t, $J = 7.2$ Hz, 2H), 3.99 (t, $J = 7.6$ Hz, 2H), 7.40 (d, $J = 6.8$ Hz, 2H), 7.54–7.66 (m, 5H), 8.40 (d, $J = 7.2$ Hz, 2H), 9.40 (s, 1H), 9.60 ppm (s, 1H); ^{13}C NMR (100 MHz, [D$_6$]DMSO): $\delta = 38.3$, 46.2, 124.7, 125.6 (2C), 126.0 (2C), 126.7 (2C), 130.7, 132.6, 133.8, 136.7, 144.3, 149.9, 165.6, 175.0, 176.6, 181.6 ppm; MS (ES, 70 eV): *m/z* 447 $[M+H]^+$; elemental analysis: calcd (%) for $C_{19}H_{15}ClN_4O_3S_2$: C 51.06, H 3.38, N 12.54; found: C 51.11, H 3.39, N 12.61.

(*Z*)-*N*′-(3-(5-(4-Chlorobenzylidene)-4-oxo-2-thioxothiazolidin-3-yl)propanoyl)-1-naphthohydrazide (6): Yield: 70%; mp: 269–270 °C; ^{1}H NMR (400 MHz, $CDCl_3$): $\delta = 2.32$ (t, $J = 7.6$ Hz, 2H), 3.91 (t, $J = 7.2$ Hz, 2H), 7.39 (d, $J = 8.8$ Hz, 2H), 7.54–7.63 (m, 6H), 7.80–8.10 (m, 4H), 9.60 ppm (br s, 2H); ^{13}C NMR (100 MHz, $CDCl_3$): $\delta = 39.3$, 44.9, 121.7, 124.0, 124.7, 125.1, 125.7, 126.6 (2C), 129.5 (2C), 132.6, 132.7, 133.8, 134.5, 136.4, 137.6, 138.7, 143.3, 145.9, 164.6, 169.0, 176.9, 178.6 ppm; MS (ES, 70 eV): *m/z* 496 $[M+H]^+$; elemental analysis: calcd (%) for $C_{24}H_{18}ClN_3O_3S_2$: C 58.12, H 3.66, N 8.47; found: C 58.17, H 3.71, N 8.53.

(*Z*)-*N*′-(3-(5-(4-Chlorobenzylidene)-4-oxo-2-thioxothiazolidin-3-yl)propanoyl)nicotinohydrazide (7): Yield: 89%; mp: 246–247 °C; ^{1}H NMR (400 MHz, [D$_6$]DMSO): $\delta = 2.40$ (t, $J = 8.0$ Hz, 2H), 4.12 (t, $J = 8.4$ Hz, 2H), 7.45 (d, $J = 8.4$ Hz, 2H), 7.60–7.81 (m, 4H), 8.10 (d, $J = 7.2$ Hz, 1H), 8.40 (d, $J = 7.6$ Hz, 1H), 8.80 (s, 1H), 9.40 (s, 1H), 9.60 ppm (s, 1H); ^{13}C NMR (100 MHz, [D$_6$]DMSO): $\delta = 37.8$, 47.2, 123.7, 124.4, 125.6, 126.3 (2C), 127.5 (2C), 132.2, 133.5, 136.4, 137.7, 145.3, 147.6, 164.6, 172.5, 177.4, 180.7 ppm; MS (ES, 70 eV): *m/z* 447 $[M+H]^+$; elemental analysis: calcd (%) for $C_{19}H_{15}ClN_4O_3S_2$: C 51.06, H 3.38, N 12.54; found: C 51.14, H 3.42, N 12.63.

(*Z*)-*N*′-(3-(4-Oxo-2-thioxo-5-(3,4,5-trimethoxybenzylidene)thiazolidin-3-yl)propanoyl)benzohydrazide (8): Yield: 86%; mp: 245–247 °C; ^{1}H NMR (400 MHz, [D$_6$]DMSO): $\delta = 2.52$ (t, $J = 7.6$ Hz, 2H),

3.90 (s, 9H), 4.23 (t, J=8.0 Hz, 2H), 7.11 (s, 2H), 7.40 (s, 1H), 7.65–7.72 (m, 3H), 7.90 (d, J=7.2 Hz, 2H), 9.72 (s, 1H), 9.81 ppm (s, 1H); ^{13}C NMR (100 MHz, [D$_6$]DMSO): δ=38.3, 49.2, 56.4, 61.2 (2C), 123.9, 124.4, 125.3 (2C), 126.6, 127.2 (2C), 127.8, 132.7, 133.9, 134.5, 138.6, 144.3, 145.6, 164.6, 168.5, 172.4, 176.7 ppm; MS (ES, 70 eV): m/z 502 $[M+H]^+$; elemental analysis: calcd (%) for $C_{23}H_{23}N_3O_6S_2$: C 55.08, H 4.62, N 8.38; found: C 55.14, H 4.72, N 8.40.

(*Z*)-*N*′-(3-(4-Oxo-2-thioxo-5-(3,4,5-trimethoxybenzylidene)thiazolidin-3-yl)propanoyl)isonicotinohydrazide (9): Yield: 92%; mp: 196–198 °C; ^{1}H NMR (400 MHz, [D$_6$]DMSO): δ=2.49 (t, J=7.6 Hz, 2H), 3.93 (s, 9H), 4.32 (t, J=8.0 Hz, 2H), 7.23 (s, 2H), 7.60 (s, 1H), 7.90 (d, J=7.8 Hz, 2H), 8.40 (d, J=8.0 Hz, 2H), 9.61 (s, 1H), 9.72 ppm (s, 1H); ^{13}C NMR (100 MHz, [D$_6$]DMSO): δ=39.4, 48.6, 57.4, 59.8 (2C), 123.4, 124.1, 124.9 (2C), 125.1, 126.2, 126.6, 132.3, 133.1, 133.4, 137.4, 143.2, 144.5, 164.3, 169.4, 174.6, 178.7 ppm; MS (ES, 70 eV): m/z 503 $[M+H]^+$; elemental analysis: calcd (%) for $C_{22}H_{22}N_4O_6S_2$: C 52.58, H 4.41, N 11.15; found: C 52.64, H 4.52, N 11.23.

(*Z*)-*N*′-(3-(4-Oxo-2-thioxo-5-(3,4,5-trimethoxybenzylidene)thiazolidin-3-yl)propanoyl)-1-naphthohydrazide (10): Yield: 75%; mp: 238–240 °C; ^{1}H NMR (400 MHz, CDCl$_3$): δ=2.36 (t, J=8.4 Hz, 2H), 3.79 (s, 9H), 4.27 (t, J=8.0 Hz, 2H), 7.19 (s, 2H), 7.65–7.80 (m, 3H), 8.13–8.85 (m, 5H), 10.20 ppm (br s, 2H); ^{13}C NMR (100 MHz, CDCl$_3$): δ=37.9, 49.6, 57.8 (3C), 121.4, 123.1, 124.3 (2C), 125.4, 126.0, 126.6, 127.2, 127.6, 128.3, 129.5, 132.1, 132.7, 133.0, 133.4, 138.2, 141.2, 143.6, 166.3, 171.7, 172.6, 180.7 ppm; MS (ES, 70 eV): m/z 552 $[M+H]^+$; elemental analysis: calcd (%) for $C_{27}H_{25}N_3O_6S_2$: C 58.79, H 4.57, N 7.62; found: C 58.84, H 4.62, N 7.73.

(*Z*)-*N*′-(3-(4-Oxo-2-thioxo-5-(3,4,5-trimethoxybenzylidene)thiazolidin-3-yl)propanoyl)nicotinohydrazide (11): Yield: 84%; mp: 234–236 °C; ^{1}H NMR (400 MHz, [D$_6$]DMSO): δ=2.34 (t, J=8.4 Hz, 2H), 3.87 (s, 9H), 4.19 (t, J=7.6 Hz, 2H), 7.21 (s, 2H), 7.54 (s, 1H), 7.60 (t, J=8.8 Hz, 1H), 8.10 (s, 1H), 8.64 (s, 1H), 8.71 (s, 1H), 9.61 ppm (d, J=11.2 Hz, 2H); ^{13}C NMR (100 MHz, [D$_6$]DMSO): δ=40.0, 49.3, 56.7, 58.3 (2C), 121.9, 123.6, 124.2 (2C), 124.9, 125.6, 126.1, 132.5, 132.9, 133.9, 138.6, 142.5, 144.8, 163.9, 169.1, 174.2, 177.9 ppm; MS (ES, 70 eV): m/z 503 $[M+H]^+$; elemental analysis: calcd (%) for $C_{22}H_{22}N_4O_6S_2$: C 52.58, H 4.41, N 11.15; found: C 52.62, H 448, N 11.21.

(*Z*)-*N*′-(3-(5-(4-Nitrobenzylidene)-4-oxo-2-thioxothiazolidin-3-yl)propanoyl)benzohydrazide (12): Yield: 69%; mp: 248–249 °C; ^{1}H NMR (400 MHz, [D$_6$]DMSO): δ=2.54 (t, J=8.8 Hz, 2H), 4.12 (t, J=8.4 Hz, 2H), 7.63–7.83 (m, 7H), 7.92 (s, 1H), 8.31 (d, J=9.6 Hz, 2H), 9.60 ppm (d, J=11.6 Hz, 2H); ^{13}C NMR (100 MHz, [D$_6$]DMSO): δ=38.1, 46.9, 120.1, 120.6, 121.9 (2C), 125.4, 126.1, 126.6, 133.9, 134.6, 135.4, 139.6, 141.6, 143.0, 143.5, 163.4, 168.5, 173.2, 174.9 ppm; MS (ES, 70 eV): m/z 457 $[M+H]^+$; elemental analysis: calcd (%) for $C_{20}H_{16}N_4O_5S_2$: C 52.62, H 3.53, N 12.27; found: C 52.72, H 3.59, N 12.31.

(*Z*)-*N*′-(3-(5-(4-Nitrobenzylidene)-4-oxo-2-thioxothiazolidin-3-yl)propanoyl)isonicotinohydrazide (13): Yield: 72%; mp: 229–231 °C; ^{1}H NMR (400 MHz, [D$_6$]DMSO): δ=2.61 (t, J=8.4 Hz, 2H), 4.23 (t, J=7.6 Hz, 2H), 7.63–7.72 (m, 4H), 7.81 (d, J=7.4 Hz, 2H), 8.03 (s, 1H), 8.22 (d, J=7.8 Hz, 2H), 10.11 ppm (d, J=11.6 Hz, 2H); ^{13}C NMR (100 MHz, [D$_6$]DMSO): δ=34.8, 45.9, 121.1, 121.7, 123.4, 125.6, 126.0, 126.8, 134.2, 134.7, 136.4, 139.9, 143.7, 144.0, 145.7, 162.8, 167.4, 174.6, 176.3 ppm; MS (ES, 70 eV): m/z 458 $[M+H]^+$; elemental analysis: calcd (%) for $C_{19}H_{15}N_5O_5S_2$: C 49.88, H 3.30, N 15.31; found: C 49.92, H 3.39, N 15.36.

(*Z*)-*N*′-(3-(5-(4-Nitrobenzylidene)-4-oxo-2-thioxothiazolidin-3-yl)propanoyl)-1-naphthohydrazide (14): Yield: 81%; mp: 263–264 °C; ^{1}H NMR (400 MHz, [D$_6$]DMSO): δ=2.50 (t, J=8.0 Hz, 2H), 4.21 (t, J=7.6 Hz, 2H), 7.92–7.72 (m, 10H), 8.10 (d, J=10.0 Hz, 2H), 9.70 ppm (d, J=12.0 Hz, 2H); ^{13}C NMR (100 MHz, [D$_6$]DMSO): δ=36.9, 46.3, 121.2, 121.6, 123.4, 124.2, 124.8, 125.3, 125.9, 126.4, 126.8, 133.4, 134.6, 135.4, 136.7, 137.7, 138.8, 143.3, 144.3, 145.8, 164.6, 166.9, 172.8, 177.3 ppm; MS (ES, 70 eV): m/z 507 $[M+H]^+$; elemental analysis: calcd (%) for $C_{24}H_{18}N_4O_5S_2$: C 56.91, H 3.58, N 11.06; found: C 56.97, H 3.62, N 11.16.

(*Z*)-*N*′-(3-(5-(4-Nitrobenzylidene)-4-oxo-2-thioxothiazolidin-3-yl)propanoyl)nicotinohydrazide (15): Yield: 72%; mp: 264–265 °C; ^{1}H NMR (400 MHz, CDCl$_3$): δ=2.41 (t, J=8.4 Hz, 2H), 4.30 (t, J=8.4 Hz, 2H), 8.01–7.81 (m, 6H), 8.13 (d, J=9.6 Hz, 2H), 8.70 (s, 1H), 10.21 ppm (d, J=11.6 Hz, 2H); ^{13}C NMR (100 MHz, CDCl$_3$): δ=36.5, 47.4, 120.1, 121.9, 124.5, 125.8, 126.4, 127.4, 134.7, 135.4, 136.6, 138.9, 143.3, 145.3, 145.9, 163.6, 165.3, 176.6, 178.7 ppm:; MS (ES, 70 eV): m/z 458 $[M+H]^+$; elemental analysis: calcd (%) for $C_{19}H_{15}N_5O_5S_2$: C 49.88, H 3.30, N 15.31; found: C 49.90, H 3.36, N 15.37.

(*Z*)-*N*′-(3-(5-(4-(Benzyloxy)benzylidene)-4-oxo-2-thioxothiazolidin-3-yl)propanoyl)benzohydrazide (16): Yield: 70%; mp: 223–224 °C; ^{1}H NMR (400 MHz, [D$_6$]DMSO): δ=2.46 (t, J=7.6 Hz, 2H), 4.21 (t, J=8.0 Hz, 2H), 5.20 (s, 2H), 7.20–7.62 (m, 13H), 7.90 (d, J=9.2 Hz, 2H), 9.72 ppm (d, J=12.4 Hz, 2H); ^{13}C NMR (100 MHz, [D$_6$]DMSO): δ=36.5, 47.4, 72.9, 121.2 (2C), 124.2 (2C), 125.8 (2C), 126.2 (2C), 127.6, 134.7 (2C), 135.4, 136.0, 136.6, 137.0, 138.9, 141.4, 143.8, 144.3, 145.4, 166.9, 168.3, 179.6, 182.7 ppm; MS (ES, 70 eV): m/z 518 $[M+H]^+$; elemental analysis: calcd (%) for $C_{27}H_{23}N_3O_4S_2$: C 62.65, H 4.48, N 8.12; found: C 62.70, H 4.56, N 8.16.

(*Z*)-*N*′-(3-(5-(4-(Benzyloxy)benzylidene)-4-oxo-2-thioxothiazolidin-3-yl)propanoyl)isonicotinohydrazide (17): Yield: 79%; mp: 233–234 °C; ^{1}H NMR (400 MHz, CDCl$_3$): δ=2.38 (t, J=7.6 Hz, 2H), 4.12 (t, J=8.0 Hz, 2H), 5.11 (s, 2H), 7.18–7.35 (m, 7H), 7.63–7.72 (m, 3H), 7.92 (d, J=7.6 Hz, 2H), 8.31 (d, J=7.2 Hz, 2H), 9.93 ppm (d, J=12.4 Hz, 2H); ^{13}C NMR (100 MHz, [D$_6$]DMSO): δ=180.7, 178.4, 166.3, 162.9, 143.5, 142.3, 142.0, 141.6, 139.5, 138.3, 136.9, 136.4, 135.6, 134.4 (2C), 127.2 (2C), 125.9 (2C), 125.2, 124.7 (2C), 123.2, 72.9, 47.4, 36.5 ppm; MS (ES, 70 eV): m/z 519 $[M+H]^+$; elemental analysis: calcd (%) for $C_{26}H_{22}N_4O_4S_2$: C 60.21, H 4.28, N 10.80; found: C 60.26, H 4.36, N 10.92.

(*Z*)-*N*′-(3-(5-(4-(Benzyloxy)benzylidene)-4-oxo-2-thioxothiazolidin-3-yl)propanoyl)-1-naphthohydrazide (18): Yield: 90%; mp: 240–242 °C; ^{1}H NMR (400 MHz, [D$_6$]DMSO): δ=2.43 (t, J=8.4 Hz, 2H), 4.21 (t, J=8.8 Hz, 2H), 5.12 (s, 2H), 7.36–7.20 (m, 5H), 7.92–7.62 (m, 8H), 8.44–8.31 (m, 4H), 10.17 ppm (d, J=12.8 Hz, 2H); ^{13}C NMR (100 MHz, [D$_6$]DMSO): δ=38.3, 49.4, 69.6, 123.2, 124.7 (2C), 125.2, 125.9 (2C), 126.4, 127.5, 128.2 (2C), 129.4, 132.5 (2C), 133.3 (2C), 135.6, 136.2, 136.9, 139.3, 140.7, 141.3, 141.7, 142.1, 143.3, 162.5, 164.3, 177.4, 179.7 ppm; MS (ES, 70 eV): m/z 568 $[M+H]^+$; elemental analysis: calcd (%) for $C_{31}H_{25}N_3O_4S_2$: C 65.59, H 4.44, N 7.40; found: C 65.66, H 4.46, N 7.42.

(*Z*)-*N*′-(3-(5-(4-(Benzyloxy)benzylidene)-4-oxo-2-thioxothiazolidin-3-yl)propanoyl)nicotinohydrazide (19): Yield: 79%; mp: 249–250 °C; ^{1}H NMR (400 MHz, [D$_6$]DMSO): δ=2.34 (t, J=7.6 Hz, 2H), 4.09 (t, J=8.0 Hz, 2H), 5.17 (s, 2H), 7.11–7.23 (m, 5H), 7.91–8.12 (m, 7H), 8.62 (d, J=6.0 Hz, 1H), 8.80 (s, 1H), 9.92 ppm (d, J=12.4 Hz, 2H); ^{13}C NMR (100 MHz, [D$_6$]DMSO): δ=37.6, 48.2, 73.5, 123.7, 124.1 (2C), 124.6, 126.3 (2C), 127.2, 134.2 (2C), 135.3, 136.0, 136.4, 137.3, 138.4, 141.8, 142.4, 142.6, 144.3, 164.1, 167.5, 179.6,

180.4 ppm; MS (ES, 70 eV): *m/z* 519 $[M+H]^+$; elemental analysis: calcd (%) for $C_{26}H_{22}N_4O_4S_2$: C 60.21, H 4.28, N 10.80; found: C 60.24, H 4.32, N 10.88.

Biological assays

Protein expression and Mtb PS screening: The *Mtb panC* gene (Rv3602c) encoding the PS was cloned and transformed into BL21(DE3) cells and the expression of the protein was performed as reported.[6] For the assay, in a 96-well plate, the reaction mixture was made up of PS (60 μL) with 0.4 mM NADH, 5 mM pantoic acid, 10 mM $MgCl_2$, 5 mM β-alanine, 10 mM ATP, 1 mM potassium phosphoenolpyruvate, and an enzyme mixture (20 μL) consisting of 18 units mL^{-1} each of chicken muscle myokinase, rabbit muscle pyruvate kinase and rabbit muscle lactate dehydrogenase diluted in 100 mM 2-[4-(2-hydroxyethyl)-1-piperazinyl]ethanesulfonic acid (HEPES) buffer. *Mtb* PS (6.47 pmol) was added to the reaction mixture to a final volume of 100 μL with 100 mM HEPES buffer (pH 7.8). The compounds were then added to the plates. Enzymatic activity was measured by the rate of decrease in the production of NADH. A similar protocol was followed for testing the designed and synthesised inhibitors in various concentrations of 50, 25, 10, 5, 1, 0.5 and 0.1 μM, respectively.[19] All measurements were performed at 340 nm with a heat-controlled Perkin–Elmer Victor X3 spectrophotometer. Percent inhibitions were calculated by using Equation (1).

$$\%\,\text{Inhibition} = 100 \times \left[\frac{1-(\text{compound rate})-(\text{background rate})}{(\text{full reaction rate})-(\text{background rate})}\right] \quad (1)$$

In vitro Mtb screening: The compounds were further screened for their in vitro anti-mycobacterial activity against actively growing *Mtb* H37Rv cells by using the MABA method.[20] For estimation of the activity against dormant *Mtb* forms, dormant "non-culturable" cells obtained in potassium-deficient Sauton's medium supplemented with albumin/dextrose/catalase (ADC) and 0.05% Tween-80 (37 °C, 200 rpm)[21] were exposed to different concentrations of test compounds for seven days (37 °C, 200 rpm). The number of cells resuscitated after treatment was estimated by the MPN assay. Both the treated and untreated tenfold-diluted cell suspensions were employed in triplicate for MPN assays in ADC-supplemented diluted liquid Sauton's medium in 48-well Corning microplates at 37 °C for 30 days without agitation. MPN values were calculated by using standard statistical methods.[28]

In vitro cytotoxicity screening: The synthesised compounds were further evaluated for toxicity studies in mouse macrophage cell lines (RAW 264.7). After 72 h of exposure to the compounds, the viability was assessed on the basis of cellular conversion of MTT into a formazan product by using the Promega Cell Titer 96 non-radioactive cell proliferation assay.[26] The RAW 264.7 cells were grown in Rosewell Park Memorial Institute (RPMI) medium supplemented with 10% fetal bovine serum (FBS), penicillin (10000 units) and streptomycin (10 mg mL^{-1}) in T25 flasks to attain 80–90% confluency. Cells were scraped and seeded into wells, that is, 5000 cells per well in poly-L-lysine coated plates. The microtiter plates were incubated at 37 °C, 5% CO_2, 95% air and 100% relative humidity for 24 h prior to addition of the experimental drugs. The test compounds at 100 μM concentration were then added to the cells and incubated at 37 °C for 72 h. Later, 10 mg mL^{-1} MTT (10 μL) was added and incubated for 3 h at 37 °C. At the end of incubation, formazan crystals were formed and the media were removed from the microtiter plates. The bound crystals were subsequently dissolved by adding DMSO (100 μL). The absorbance was then read on a plate reader at a wavelength of 595 nm. Relative to the control wells, the percentage growth was calculated for each well. The percentage of cells killed was calculated from Equation (2), in which OD is optical density.

$$\%\,\text{Cells killed} = \frac{100-(\text{mean OD}_{\text{sample}})}{\text{mean OD}_{\text{day 0}}} \quad (2)$$

Biophysical characterisation by using DSF: The binding affinities of the most active compounds were evaluated by thermal shift assays, in which the native protein and protein–ligand complex are mixed in the presence of a fluorescent dye. The fluorescence of the dye increases when hydrophobic residues of the protein are exposed and reaches a maximum when the protein denatures.[27] Briefly, the native protein PS (7 μL, 0.23 mg mL^{-1}) and assay buffer (9 μL, 100 mM HEPES–NaOH, pH 7.8) were subjected to stepwise heating in a real-time PCR instrument (Bio-Rad iCycler5) from 25 to 95 °C with an increment of 0.1 °C min^{-1} in the presence of the fluorescent dye SYPRO orange (1:500) sigma. As the temperature was increased, the stability of the protein decreased and became zero at equilibrium, at which point the concentrations of folded and unfolded protein were equal, and this temperature was noted as the melting temperature. The dye exhibited the maximum fluorescence at this point because it was exposed to the hydrophobic portion of the protein as a result of the protein denaturing. A positive shift in the T_m value relative to that of the native protein indicated stabilisation of the protein–ligand complexes.

Acknowledgements

The authors are thankful to the Department of Science and Technology, New Delhi, India (SR/S1/OC-70/2010) and the Program of the Presidium of the Russian Academy of Sciences "Molecular and Cellular Biology" for financial assistance. We also acknowledge Dr. David Eisenberg and Dr. Shuishu Wang, Department of Biochemistry and Molecular Biology, USUHS, Maryland (USA), for providing the Mtb PS clone. D.S. acknowledges the University Grants Commission, New Delhi, India, for a UGC Research Award.

Keywords: drug design · enzymes · inhibitors · thiazolidines · tuberculosis

[1] World Health Organization (WHO), *Global Tuberculosis Report*, **2013**, http://www.who.int/tb/publications/global_report/en/.
[2] R. Singh, Rajni, A. Meena, L. S. Meena, *J. Bacteriol. Parasit.* **2011**, *2*, 105.
[3] World Health Organization (WHO), *"Totally drug-resistant" tuberculosis: A WHO consultation on the diagnostic definition and treatment options*, **2012**, http://www.who.int/tb/challenges/xdr/xdrconsultation/en/.
[4] R. Zheng, J. S. Blanchard, *Biochemistry* **2001**, *40*, 12904–12912.
[5] V. K. Sambandamurthy, X. Wang, B. Chen, R. G. Russell, S. Derrick, F. M. Collins, S. L. Morris, W. R. Jacobs, Jr., *Nat. Med.* **2002**, *8*, 1171–1174.
[6] S. Wang, D. Eisenberg, *Protein Sci.* **2003**, *12*, 1097–1107.
[7] S. Wang, D. Eisenberg, *Biochemistry* **2006**, *45*, 1554–1561.
[8] A. W. Hung, H. L. Silvestre, S. Wen, A. Ciulli, T. L. Blundell, C. Abell, *Angew. Chem. Int. Ed.* **2009**, *48*, 8452–8456; *Angew. Chem.* **2009**, *121*, 8604–8608.
[9] D. E. Scott, G. J. Dawes, M. Ando, C. Abell, A. Ciulli, *ChemBioChem* **2009**, *10*, 2772–2779.
[10] H. L. Silvestre, T. L. Blundell, C. Abell, A. Ciulli, *Proc. Natl. Acad. Sci. USA* **2013**, *110*, 12984–12989.

[11] Schrödinger Suite 2011, Protein Preparation Wizard, Maestro version 9.2, Glide version 5.7, Phase version 3.0, LigPrep version 2.5, Epik version 2.2, Schrödinger LLC, New York, NY (USA), **2011**.
[12] S. L. Dixon, A. M. Smondyrev, S. N. Rao, *Chem. Biol. Drug Des.* **2006**, *67*, 370 – 372.
[13] N. K. Salam, R. Nuti, W. Sherman, *J. Chem. Inf. Model.* **2009**, *49*, 2356 – 2368.
[14] ASINEX, ASINEX Platinum Collection, Winston-Salem, NC (USA), http://www.asinex.com.
[15] R. A. Friesner, J. L. Banks, R. B. Murphy, T. A. Halgren, J. J. Klicic, D. T. Minz, M. P. Repasky, E. H. Knoll, M. Shelley, J. K. Perry, D. E. Shaw, P. Francis, P. S. Shenkin, *J. Med. Chem.* **2004**, *47*, 1739 – 1749.
[16] M. D. Eldridge, C. W. Murray, T. R. Auton, G. V. Paolini, R. P. Mee, *J. Comput. Aid. Mol. Des.* **1997**, *11*, 425 – 445.
[17] R. A. Friesner, R. B. Murphy, M. P. Repasky, L. L. Greenwood, T. A. Halgren, P. C. Sanschagrin, D. T. Minz, *J. Med. Chem.* **2006**, *49*, 6177 – 6196.
[18] R. K. Suto, T. D. McKee, T. Tibbits, J. M. Sowadski (Pintex Pharmaceuticals, Inc.), Int. PCT Pub. No. WO 2005/007123 A2, **2005**.
[19] E. L. White, K. Southworth, L. Ross, S. Cooley, R. B. Gill, M. I. Sosa, A. Manouvakhova, L. Rasmussen, C. Goulding, D. Eisenberg, T. M. Fletcher, *J. Biol. Screen.* **2006**, *12*, 100 – 102.
[20] S. G. Franzblau, R. S. Witzig, J. C. McLaughlin, P. Torres, G. Madico, A. Hernandez, M. T. Degnan, M. B. Cook, V. K. Quenzer, R. M. Ferguson, R. H. Gilman, *J. Clin. Microbiol.* **1998**, *36*, 362 – 366.
[21] E. D. Rossi, J. A. Ainsa, G. Riccardi, *FEMS Microbiol. Rev.* **2006**, *30*, 36 – 52.
[22] L. Rodrigues, J. A. Ainsa, L. Amaral, M. Viveiros, *Recent Pat. Anti-Infect. Drug Discovery* **2011**, *6*, 118 – 127.
[23] J. M. Pagès, L. Amaral, *Biochim. Biophys. Acta Proteins Proteomics* **2009**, *1794*, 826 – 833.
[24] E. Salina, O. Ryabova, A. Kaprelyants, V. Makarov, *Antimicrob. Agents Chemother.* **2014**, *58*, 55 – 60.
[25] D. J. Murphy, J. R. Brown, *BMC Infect. Dis.* **2007**, *7*, 84.
[26] J. C. De Man, *J. Appl. Microbiol.* **1975**, *1*, 67 – 78.
[27] D. A. Scudiero, R. H. Shoemaker, K. D. Paull, A. Monks, S. Tierney, T. H. Nofziger, M. J. Currens, D. Seniff, M. R. Boyd, *Cancer Res.* **1988**, *48*, 4827 – 4833.
[28] F. H. Niesen, H. Berglund, M. Vedadi, *Nat. Protoc.* **2007**, *2*, 2212 – 2221.

Received: May 2, 2014
Published online on ■■ ■■, 0000

Let sleeping cells lie: *Mycobacterium tuberculosis* pantothenate synthetase (*Mtb* PS) has become a target for new therapeutics to treat tuberculosis. Nanomolar thiazolidine inhibitors of *Mtb* PS were developed by rational inhibitor design involving modelling, in vitro screening and optimisation. Hit expansion of the lead by synthesis led to an improved inhibitor with an IC_{50} value of 350 nM and an *Mtb* MIC value of 1.55 μM. Some of these compounds also showed good activity against dormant *Mtb* cells.

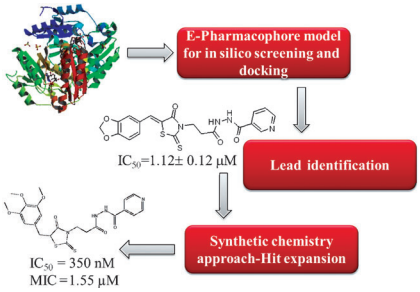

P. B. Devi, G. Samala, J. P. Sridevi, S. Saxena, M. Alvala, E. G. Salina, D. Sriram, P. Yogeeswari**

■■ – ■■

Structure-Guided Design of Thiazolidine Derivatives as *Mycobacterium tuberculosis* Pantothenate Synthetase Inhibitors